Supporting Information

Iron incorporated metal-organic frameworks for oxidative cleavage of *trans*-anethole to *p*-anisaldehyde

Jun Xiong, [a] Xin Yuan, [a] Min-Hua Zong, [a] Xiaoling Wu, * [a] and Wen-Yong Lou * [ab]

[a] *Lab of Applied Biocatalysis, National Engineering Research Center of Wheat and Corn Further Processing, School of Food Science and Engineering, South China University of Technology, No. 381 Wushan Road, Guangzhou 510640, Guangdong, China*

[b] *Guangdong Province Key Laboratory for Green Processing of Natural Products and Product Safety, South China University of Technology, No. 381 Wushan Road, Guangzhou 510640, Guangdong, China*

* Correspondence to: Lab of Applied Biocatalysis, School of Food Science and Engineering, South China University of Technology, Guangzhou 510640, China
E-mail: wuxl18@scut.edu.cn (Xiaoling Wu); wylou@scut.edu.cn (Wen-Yong Lou)

Experimental details

Chemicals.

Zinc nitrate hexahydrate ($Zn(NO_3)_2 \cdot 6H_2O$), iron(III) chloride hexahydrate ($FeCl_3 \cdot 6H_2O$), iron(III) trifluoromethanesulfonate ($Fe(OTf)_3$), iron(III) nitrate nonahydrate ($Fe(NO_3)_3 \cdot 9H_2O$), iron(III) sulfate hydrate ($Fe_2(SO_4)_3 \cdot H_2O$), iron(III) acetate ($Fe(OAc)_3$), iron(III) citrate dihydrate (FeCA), iron(II) chloride tetrahydrate ($FeCl_2 \cdot 4H_2O$), copper(II) chloride dihydrate ($CuCl_2 \cdot 2H_2O$), cobalt chloride hexahydrate ($CoCl_2 \cdot 6H_2O$), manganese(II) chloride ($MnCl_2$) and nickel(II) chloride ($NiCl_2$) were obtained from Aladdin Co., Ltd. 2,2'-bipyridine-5,5'-dicarboxylic acid, 2,2'-bipyridine-3,3'-dicarboxylic acid, 2,2'-bipyridine-4,4'-dicarboxylic acid and 2,2'-bipyridine-6,6'-dicarboxylic acid were purchased from Admas Co., Ltd. *Trans*-anethole and *p*-anisaldehyde were bought from TCI (Shanghai) Development Co., Ltd. Organic solvents including acetonitrile, methanol, *N,N*-dimethylacetamide (DMA), cyclohexane, n-heptane, n-octane, isooctane, n-decane, tert-butanol, tert-amylalcohol and methylbenzene were purchased from Damao Chemical Reagent Factory.

Fabrication of Zn-bpydc·Fe.

Firstly, the Fe^{3+} coordinated bpydc ligand (bpydc·Fe) was prepared. In a 100 mL glass bottle, 2,2′-bipyridine-5,5′-dicarboxylic acid (bpydc, 0.5 mmol, 122.1 mg) and $FeCl_3 \cdot 6H_2O$ (1 mmol, 270.3 mg) were dispersed in 5 mL of acetonitrile and stirred under room temperature. After 12 h, the suspension was then separated by filtration and the solid product was collected and washed with acetonitrile 3 times before being dried under 60 °C to afford brown powdery bpydc·Fe.

MOFs catalyst Zn-bpydc·Fe was synthesized through solvothermal method. Typically, 10 mL of DMA containing 24.42 mg of bpydc·Fe and 0.2 mmol of $Zn(NO_3)_2 \cdot 6H_2O$ was placed in a 25 mL reactor and heated at 100 °C for 24 h. After cooling down to room temperature, the light brown powder of Zn-bpydc·Fe was separated by filtration and washed with DMA and methanol in sequence followed by drying at 60 °C over night.

Zn-bpydc was similarly synthesized with bpydc in place of bpydc·Fe.

Characterizations.

Scanning electron microscopy (SEM) images of samples were taken on a field emission gun scanning electron microscope (HITACHI UHRFE-SEM SU8200) at an accelerating voltage of 5.0 kV. Transmission electron microscopy (TEM) images were taken on a JEOL JEM-2010 high-resolution transmission electron microscope with an accelerating voltage of 120 kV. X-ray diffraction (XRD) patterns were recorded using a Bruker D8 Advance X-Ray diffractometer with a Cu Kα anode (λ =0.15406 nm) at 40 kV and 40 mA with step size of 5°/min. Fourier transform infrared (FTIR) analysis was carried out on a TENSOR27/HYPERION Bruker spectrometer in transmission mode 64 scans were performed with 1 cm^{-1} interval. UV spectra were recorded on a Shimadzu UV-2550 UV-VIS spectrophotometer. Nitrogen sorption analysis was performed on an automatic surface area and porosity analyzer (Micromeritics ASAP 2460) at 77 K. The samples (at least 100 mg) were degassed at 150 °C for 10 h before isotherm measurement. Brunauer-Emmett-Teller (BET) surface area were calculated based on the adsorption branch. Pore size distribution was analyzed using the density function theory (DFT) method. The content of Fe and Zn in the samples were detected by inductively coupled plasma atomic emission spectrometry (ICP-AES) analysis which was performed on a PerkinElmer Optima 8300 instrument. Thermogravimetric

analysis (TGA) in air was performed on a TA Instruments TGA 2050 Thermogravimetric Analyzer. Samples were heated from room temperature to 600 °C at a rate of 20 °C/min. X-ray photoelectron spectroscopy (XPS) was performed on a Kratos Axis Ulra DLD spectrometer using a Mg Kα radiation (10 kV, 20 mA) as energy source. The content of C and N was measured on Elemental analyzer (Vario EL cube) instrument.

Zn-bpydc·Fe catalyzed oxidative cleavage of *trans*-anethole

For a typical reaction, 10 mg of Zn-bpydc·Fe was added to a 10 mL glass tube containing 0.2 M of *trans*-anethole in 2 mL of organic solvents. The reaction tube was degassed with oxygen (0.1 MPa) 3 times and kept under oxygen (0.1 MPa) by using a balloon. The reaction system was magnetic stirred at 50-70 °C to start the reaction. At different time intervals, samples were taken for HPLC analysis. The yield was calculated as the percentage molar ratio of the *p*-anisaldehyde produced to the total *trans*-anethole added to the reaction system. An Agilent Technologies 1260 Infinity HPLC system equipped with a UV index detector (1260 DAD VL) and a 150 × 4.6 mm, 5 μm inertsil ODSSP column (GL Sciences, Inc, Japan) was used for HPLC analysis. Typically, 10 μL of sample was injected, and 70% methanol (v/v) was employed as the mobile phase with a flow rate of 1.0 $mL \cdot min^{-1}$, operated at 35 °C. The absorbance at 260 nm (for *trans*-anethole) and 275 nm (for *p*-anisaldehyde) was recorded within 10 min.

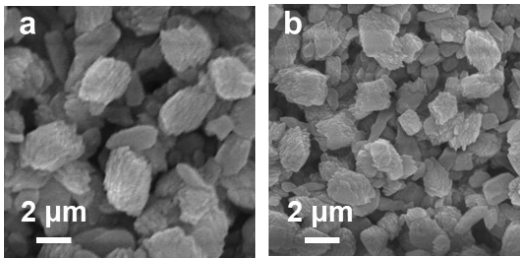

Fig. S1. SEM images of Zn-bpydc (a) and Zn-bpydc·Fe (b) under low magnification.

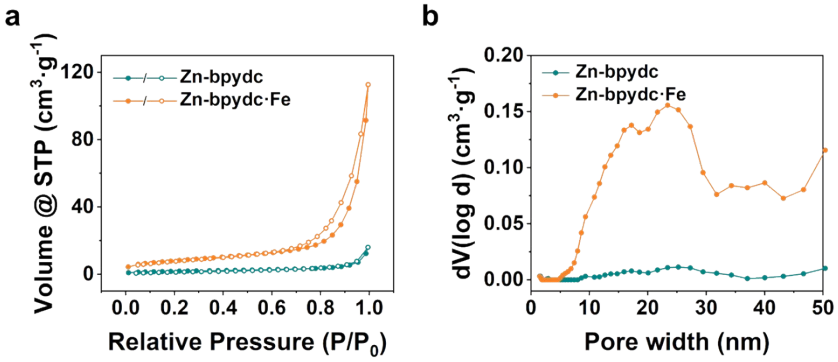

Fig. S2. Nitrogen sorption isotherm (a) and pore size distribution calculated based on the density functional theory model (b) of Zn-bpydc and Zn-bpydc·Fe, respectively.

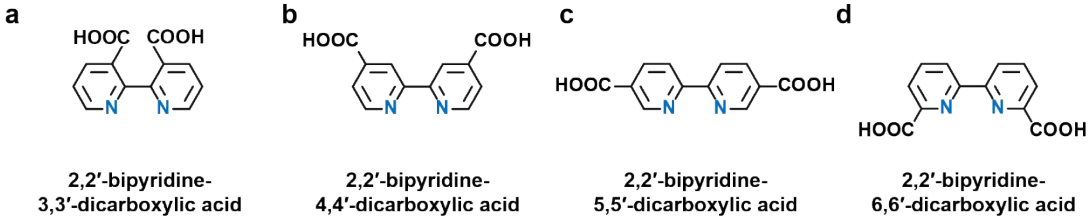

Fig. S3. Chemical structures of bipyridine dicarboxylic acids (bpydc) with different conformations, 2,2′-bipyridine-3,3′-dicarboxylic acid (a), 2,2′-bipyridine-4,4′-dicarboxylic acid (b), 2,2′-bipyridine-5,5′-dicarboxylic acid (c) and 2,2′-bipyridine-6,6′-dicarboxylic acid (d).

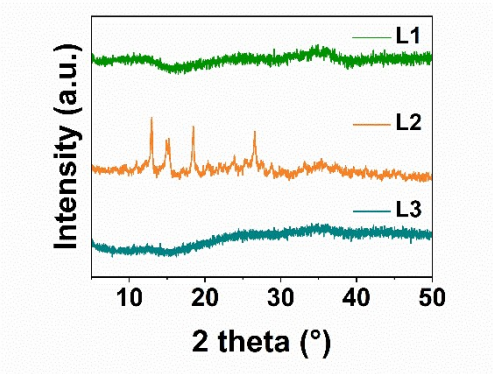

Fig. S4. XRD patterns of Zn-bpydc·Fe with different ligands (L1: 2,2′-bipyridine-4,4′-dicarboxylic acid; L2: 2,2′-bipyridine-5,5′-dicarboxylic acid; L3: 2,2′-bipyridine-6,6′-dicarboxylic acid).

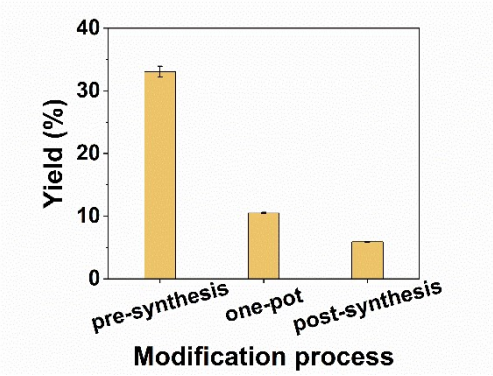

Fig. S5. Effect of the methods of Fe incorporation on the activity of Zn-bpydc·Fe.

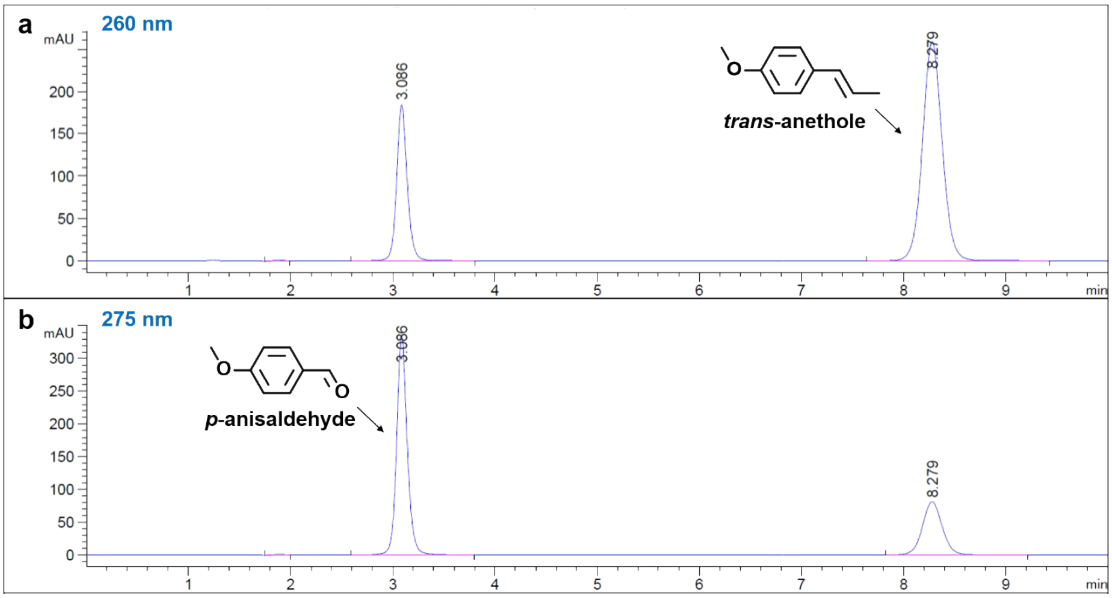

Fig. S6. HPLC chromatograms of the substrate *trans*-anethole (a) and the product *p*-anisaldehyde (b).

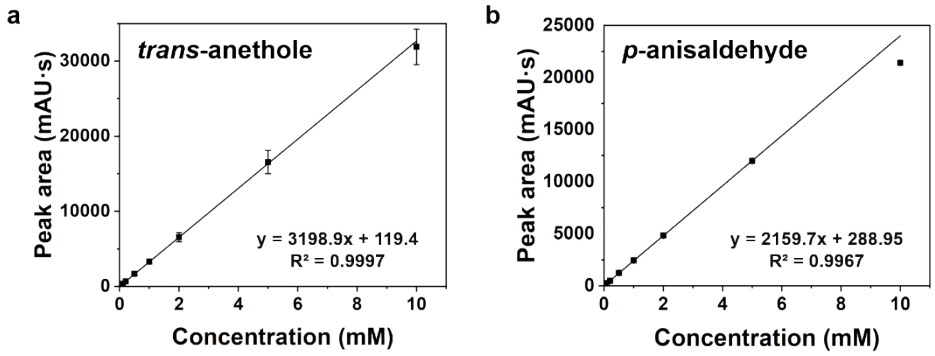

Fig. S7. Calibration curves of the substrate *trans*-anethole (a) and the product *p*-anisaldehyde (b).

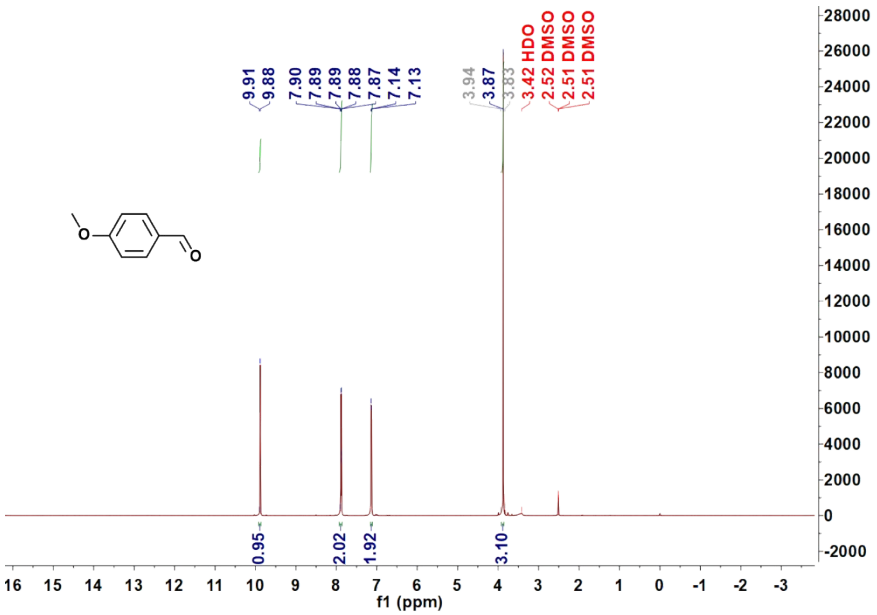

Fig. S8. ^{1}H NMR spectra of the product *p*-anisaldehyde.

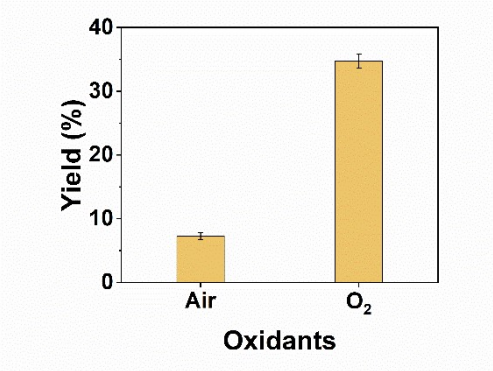

Fig. S9. Effect of oxidants on the yield of *p*-anisaldehyde.

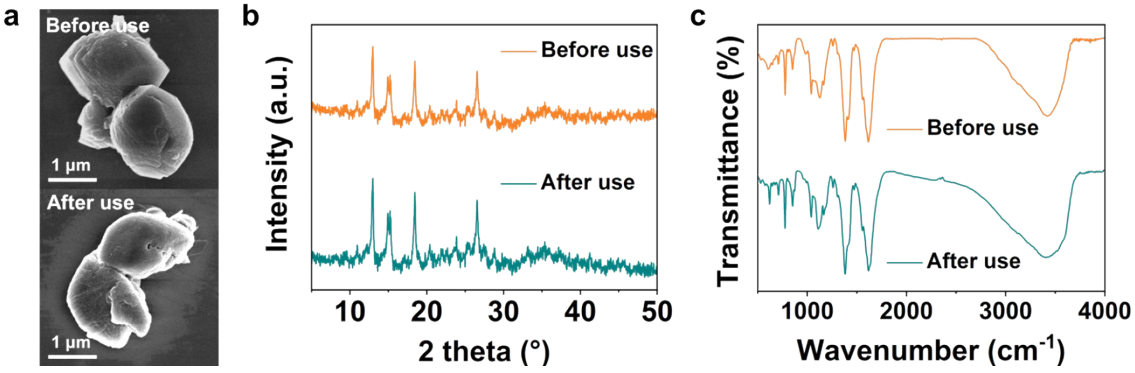

Fig. S10. SEM images (a), XRD patterns (b) and FTIR spectra (c) of Zn-bpydc·Fe before and after use.

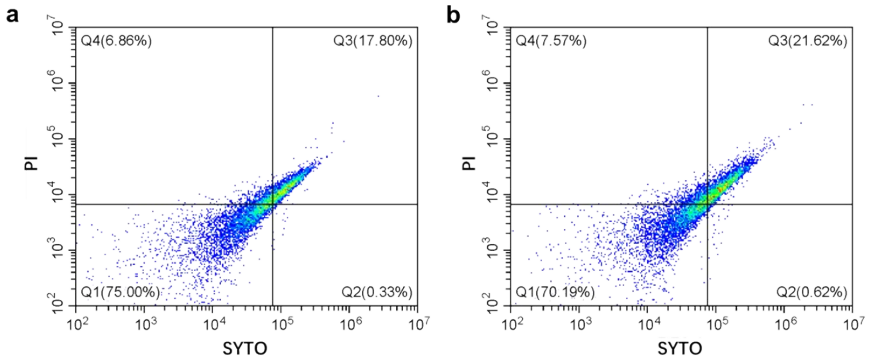

Fig. S11. Flow cytometry for *Escherichia coli* cell death analysis using SYTO and PI staining.

Table S1. BET surface area and pore volume of Zn-bpydc and Zn-bpydc·Fe.

Sample	BET surface area ($m^2 \cdot g^{-1}$)	Pore volume ($cm^3 \cdot g^{-1}$ STP)
Zn-bpydc	6.26	0.025
Zn-bpydc·Fe	28.96	0.174

Table S2. The price of the precursors of Zn-bpydc·Fe and native enzymes.

Reagents	Price (RMB·g^{-1})	Brand
Zinc nitrate hexahydrate	3.48	Aladdin
Iron(III) chloride hexahydrate	4.36	Aladdin
2,2′-bipyridine-5,5′-dicarboxylic acid	73.9	Admas
Lipoxygenase	>8000	Sigma-aldrich
Lipoxygenase	>4500	Aladdin
Lipoxygenase	>7300	Abcam